Supplementary Information:

Table S1: T3SS proteins in various families of T3SS and the flagellum.

Injectisomes				**Flagella**	**Structure/ function**	**Location**
Shigella	***Salmonella* SPI-1**	***Yersinia***	***P. syringae***			
Spa33	SpaO	YscQ	HrcQA/B	FliM/N	'Pods'; C ring	cytoplasm
MxiN	OrgB	YscL	HrpE	FliH	Stabilization of ATPase location	cytoplasm
MxiK	OrgA	YscK	HrpD	-		cytoplasm
Spa47	InvC	YscN	HrcN	FliI	ATPase	cytoplasm
Spa13	InvI	YscO	HrpO	FliJ	ATPase-associated stalk	cytoplasm
Spa24	SpaP	YscR	HrcR	FliP	export apparatus protein	cytoplasmic membrane
Spa9	SpaQ	YscS	HrcS	FliQ	export apparatus protein	cytoplasmic membrane
Spa29	SpaR	YscT	HrcT	FliR	export apparatus protein	cytoplasmic membrane
Spa40	SpaS	YscU	HrcU	FlhB	export apparatus protein	cytoplasmic membrane with large cytoplasmic domain
MxiA	InvA	YscV	HrcV	FlhA	export apparatus protein	cytoplasmic membrane with large cytoplasmic domain
MxiD	InvG	YscC	HrcC	-	secretin	outer membrane
MxiG	PrgH	YscD	HrpQ	-	MS ring?	cytoplasmic membrane
MxiJ	PrgK	YscJ	HrcJ	FliF	MS ring	cytoplasmic membrane
MxiM	InvH	YscW	-	-	pilotin	outer membrane
MxiH	PrgI	YscF	HrpA	-	needle filament	external
MxiI	PrgJ	YscI	HrpB	-	inner rod	inside of basal body
Spa32	InvJ	YscP	HrpP	FliK	control needle length	inside of basal body
IpaD	SipD	LcrV	-	-	needle tip complex	tip of needle
IpaB/C	SipB/C	YopB/D	HrpK	-	hydrophobic translocator	
MxiC	InvE	YopN	HrpJ	-		

Table S2: Sequence alignment between *S. enterica* PrgH and *S. flexneri* MxiG.

```
MxiG            -MSEAKNSNLAPFRLLVKLTNG--VGDEFPLYYGNNLIVLGRTIETLEFGND-NFPEN-- 54
PrgH            METSKEKTITSPGPYIVRLLNSSLNGCEFPLLTGRTLFVVGQSDALTASGQLPDIPADSF 60
                  :. :::  :*   :*:* *.   * ****  *..*:*:*::      *:  ::* :
MxiG            IIPVTDSKSDGIIYLTISKDNICQFSDEKGEQIDINSQFNS-FEYDGISFHLKNMRE--- 110
PrgH            FIPLDHGGVNFEIQVDTDATEIILHELKEGNSESRSVQLNTPIQVGELLILIRPESEPWV 120
                :**: ..  :  * :  .  :*  .. ::*:. . . *:*: :: . : : ::   *
MxiG            -----------DKSRGHILNGMYKNHSVFFFFAV--IVVLIIIFSLSLKKDEVKEIAEII 157
PrgH            PEQPEKLETSAKKNEPRFKNGIVAALAGFFILGIGTVGTLWILNSPQRQAAELDSLLGQE 180
                          .*.. :: **:    : **::.:  : .* *: * . :  *:..:
MxiG            DDKRYGIVNTGQCNYILAETQNDAVWASVALNKTGFTKCRYILVSNKEINRIQQYINQRF 217
PrgH            KERFQVLPGRDKMLYVAAQNERDTLWARQVLARGDYDKNARVINENEENKRISIWLDTYY 240
                .::   : . .:  *: *:.:.*::**  .* : .: *   :: .*:* :**. :::  :
MxiG            PFINLYVLNLVSDKAELLVFLSKERNSSKDTELDKLKNALIVEFPYIKNIKFNYLSDHNA 277
PrgH            PQLAYYRIHFD-EPRKPVFWLSRQRNTMSKKELEVLSQKLRALMPYADSVNITLMDDVTA 299
                * :  * :::  :  : :.:**::**: ...**: *.: * . :** ..:::. :.* .*
MxiG            RGDAKGIFTKVNVQYKEICENNKVTYSVREELTDEKLELINRLISEHKNIYGDQYIEFSV 337
PrgH            AGQAEAGLKQQALPYSRRNHKGGVTFVIQGALDDVEILRARQFVDSYYRTWGGRYVQFAI 359
                 *:*:. :.:  : *..  .:. **: ::  * * ::   .::::.: . :*.:*::*::
MxiG            LLIDDDFKGKSYLNSKDSYVMLNDKHWFFLDKNK 371
PrgH            ELKDDWLKGRSFQYGAEGYIKMSPGHWYFPSPL- 392
                 * ** :**:*:  . :.*: :.  **:* .
```

The sequence identity between MxiG and PrgH is 21%. The transmembrane domain is labeled in red.

Table S3: Sequence alignment between *S. flexneri* Spa47, *S. enterica* FliI, and *T. thermophilus* V-type ATP synthase subunit B.

```
Spa47           --MSYTKLLTQLS--------FP--------NRISGPILETSLSDVSIGEICNIQAGIES 42
FliI            MTTRLTRWLTALDNFEAKMALLPAVRRYGRLTRATGLVLEATGLQLPLGATCIIERQDGP 60
V-ATPase        -MDLLKKEYTGIT-------------------YISGPLLFVENAKDLAYGAIVDIKDGTG- 40
                     .:  * :                      ::  .  ::. *    *:
Spa47           NEIVARAQVVGFHDEKTILS-------LIGNSRGLSRQTLIKPTAQFLH-TQVGRGLLGA 94
FliI            ETKEVESEVVGFNGQRLFLMPLEEVEGILPGARVYARNGHGDGLQSGKQ-LPLGPALLGR 119
V-ATPase        --RVRGGQVIEVSEEYAVIQ-------VFEETTGLDLATTSVSLVEDVARLGVSKEMLGR 91
                      .:*: .  :  .:        ::  :             .      :.  :**
Spa47           VVNPLGEVTDKFAVTDNSEILYRPVDNAPPLYSERAAIEKPFLTGIKVIDSLLTCGEGQR 154
FliI            VLDGGGKPLDGLPAPDTLETGALITPPFNPL--QRTPIEHVLDTGVRAINALLTVGRGQR 177
V-ATPase        RFNGIGKPIDGLPPITPEKRLPITGLPLNPV--ARRKPEQFIQTGISTIDVMNTLVRGQK 149
                 .:  *:  * :.     :          *:   *   *: : **: .*: : *  .**:
Spa47           MGIFASAGCGKTFLMNMLIEHSGAD-------------IYVIGLIGERGREVTETVDYLK 201
FliI            MGLFAGSGVGKSVLLGMMARYTRAD-------------VIVVGLIGERGREVKDFIENIL 224
V-ATPase        LPIFSGSGLPANEIAAQIARQATVRPDLSGEGEKEEPFAVVFAAMGITQRELSYFIQEFE 209
                : :*:.:*   . :   : . : .                *.. :*   **:.  :: :
Spa47           NSEKKSRCVLVYATSDYSSVDRCNAAYIATAIAEFFR-TEGHKVALFIDSLTRYARALRD 260
FliI            GPDGRARSVVIAAPADVSPLLRMQGAAYATRIAEDFR-DRGQHVLLIMDSLTRYAMAQRE 283
V-ATPase        RTGALSRSVLFLNKADDPTIERILTPRMALTVAEYLAFEHDYHVLVILTDMTNYCEALRE 269
                 .   :*.*:.   :* ..: *   .  *  :** :   .. :* ::: .:*.*. * *:
Spa47           VALAAGESPARRGYPVSVFDSLPRLLERPGK-LKAGGSITAFYTVLLEDDDFADPLAEEV 319
FliI            IALAIGEPPATKGYPPSVFAKLPALVERAGNGIHGGGSITAFYTVLTEGDDQQDPIADSA 343
V-ATPase        IGAAREEIPGRRGYPGYMYTDLATIYERAGVVEGKKGSVTQIPILSMPDDDRTHPIPDLT 329
                :. *  * *. :***  :: .*. : **.*      **:* :  :   .**  .*:.: .
Spa47           RSILDGHIYLSRNLAQKGQFPAIDSLKSISRVFT------QVVDEKHRIMAAAFRELLSE 373
FliI            RAILDGHIVLSRRLAEAGHYPAIDIEASISRAMT------ALITEQHYARVRLFKQLLSS 397
V-ATPase        GYITEGQIQLSRELHRKGIYPPIDPLPSLSRLMNNGVGKGKTREDHKQVSDQLYSAYANG 389
                  * :*:* ***.* . * :*.**   *:** :.          :::      :    .
Spa47           IEELRTIIDFGEYKPGENA----------------------SQDKIYNKISVVESFLKQD 411
FliI            FQRNRDLVSVGAYAKGSDP----------------------MLDKAITLWPQLEAFLQQG 435
V-ATPase        VDIRKLVAIIGEDALTENDRRYLQFADAFERFFINQGQQNRSIEESLQIAWALLSMLPQG 449
                .:  : :  .*     .:                          ::       : ::* *.
Spa47           YRLGFTYEQTMELIGETIR---------- 430
FliI            IFERADWEDSLQALDLIFPTV-------- 456
V-ATPase        ELKRISKDHIGKYYGQKLEEIWGAPQALD 478
                       :.  :  .  :
```

The sequence identity between Spa47 and FliI is 37%.

Table S4: Sequence alignment between *S. flexneri* Spa13 and *S. enterica* FliJ.

```
FliJ            -MAQHGALETLKDLAEKEVDDAARLLGEMRRGCQQAEEQLKMLIDYQNEYRSNLNTDMGN 59
Spa13           MLKIKDKYQRSVKLIEAHILTLKKKN-SLYRDVEALDKRIIYFLQLENDLEP-----VG- 53
                 :  :.  :   .* * .:    :   .: *. :  ::::  ::: :*: ..     :*

FliJ            GIASNRWINYQQFIQTLEKAIEQHRLQLTQWTQKVDLALKSWREK--KQRLQAWQTLQDR 117
Spa13           AQSVSQLFNTRRKIAIVKKHIIQYQSERILLKGRIEEIQKDIDEANASKRKLLHKESKIC 113
                . : .: :* :: *  ::* * *:: :    . :::   *.  *   .:*    :  :

FliJ            QTAAALLAENRMDQKKMDEFAQRAAMRKPE 147
Spa13           KRIGLIKRNNFAKQLILDELSQEDMKYGIR 143
                :  . :  :*  .*  :**::*.      .
```

The whole sequence of Spa13 was identified in (50). The sequence similarity between FliJ and Spa13 is 24%, and the identity is 13%.

50. Penno C*, et al.* (2006) Transcriptional slippage controls production of type III secretion apparatus components in *Shigella flexneri*. *Mol Microbiol* 62(5):1460-1468.

Table S5: Sequence alignment between *S. flexneri* Spa33 (293 aa) and *S. enterica* FliN (137 aa).

```
FliN            ------------------------------------------------------------
Spa33           MLRIKHFDANEKLQILYAKQLCERFSIQTFKNKFTGSESLVTLTSVCGDWVIRIDTLSFL 60


FliN            ------------------------------------------------------------
Spa33           KKKYEVFSGFSTQESLLHLSKCVFIESSSVFSIPELSDKITFRITNEIQYATTGSHLCCF 120


FliN            ----------------------------------------MSDMNNPSDENTGALDDLWADA 22
Spa33           SSSLGIIYFDKMPVLRNQVSLDLLHHLLEFCLGSSNVRLATLKRIRTGDIIIVQKLYNLL 180
                                                 :: ::.    :   ::.*:

FliN            LN------EKKATTNKSAADAVFQQLGGGDVSGAMQDIDLIMDIPVKLTVELGRTRMTIK 76
Spa33           LCNQVIIGDYIVNDNNEAKINLSESNGESDHTEVSLALFNYDDINVKVDFILLEKKMTIN 240
                *       :  .. *:.*   : :. * .* : .   :    ** **: . * ..:***:

FliN            ELLRLTQGSVVALDGLAGEPLDILINGYLIAQGEVVVVADKNGVRITDIITPSERMRRLS 136
Spa33           ELKMYVENELFKFPDDIVKHVNIKVNGSLVGHGELVSIEDGYGIEISSWMVKE------- 293
                **   .:..:. : .   : ::* :** *:.:**:* : * **:.*:. :. .

FliN            R 137
Spa33           -
```

The sequence identity between the C-terminal domain of Spa33 and FliN is 21%. The red residues in FliN form a hydrophobic patch (32), which forms the interaction site for FliH. Those residues, which are largely conserved in Spa33, likely form the binding site for MxiN (homology of FliH).

Table S6: Oligonucleotides used in construction of *mxiN::tetRA* and *spa33::tetRA* mutants.

P2	TGTAGGCTGGAGCTGCTTCG
mxiN fwd	TTTGGAGGGAAATTATACGCCTGTAGAAAGAAATTTGTCCCGATTAAATGATTCCGGGGATCCGTCGACC
mxiN rev	GCTGCAGAGCATTGCTTGCATTTATTTGATTAATCATTAACAGGATTCTCTGTAGGCTGGAGCTGCTTCG
mxiN check	AGGCCGCTATTCGAAGTGG
spa33 fwd	GGGAATAAAAATAATAGTACAGGATATAATGAACAGAGTGAAGAAGAATGATTCCGGGGATCCGTCGACC
spa33 rev	CGATGAGGGACATGTCACTCAGCATGAGATTACTCCTTTACCATCCAAGATGTAGGCTGGAGCTGCTTCG
spa33 check	TCTAAAACCGTCAGATCAATTTG

Table S7: Strains and tomographic data collected by using SerialEM and UCSF Tomography, respectively.

***Shigella* Strains**	**Total no. of tilt series**	**Pixel size (nm)**	**Image size**	**Drift correction?**	**Total no. of sub-tomograms**	**Estimated resolution (FSC at 0.5)**
WT minicells	387	0.445	3710x3838	Yes	4,631	2.7 nm
WT minicells	468	0.504	1855x1855	No	1,448	3.6 nm
Δ*mxiN* minicells	285	0.504	1855x1855	No	582	4.7 nm
Δ*spa33* minicells	443	0.504	1855x1855	No	409	5.0 nm
Osmotically shocked WT cells	334	0.504	1855x1855	No	754	

Three EM maps have been deposited in the EM Data Bank (http://www.ebi.ac.uk/pdbe/emdb/) with Accession Numbers EMD-2667, 2668 and 2669.

Supplementary Figures:

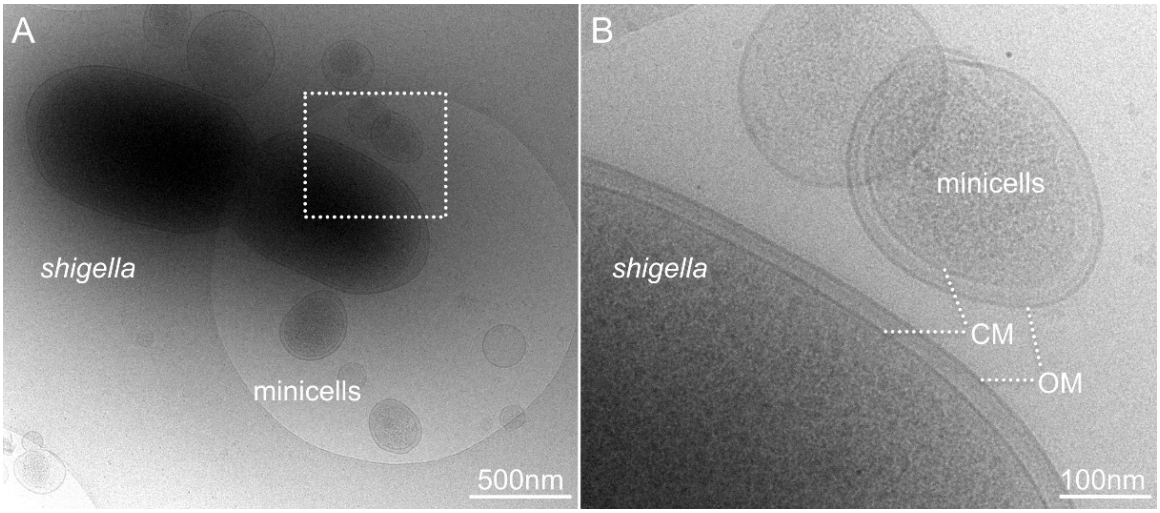

Figure S1. Cryo-EM shows regular *S. flexneri* cells and very small minicells. (A) An overview and (B) a zoomed-in view of cryo-EM image. The cell envelopes from regular cells and minicells share similar architecture which is composed of the outer membrane (OM) and the cytoplasmic membrane (CM).

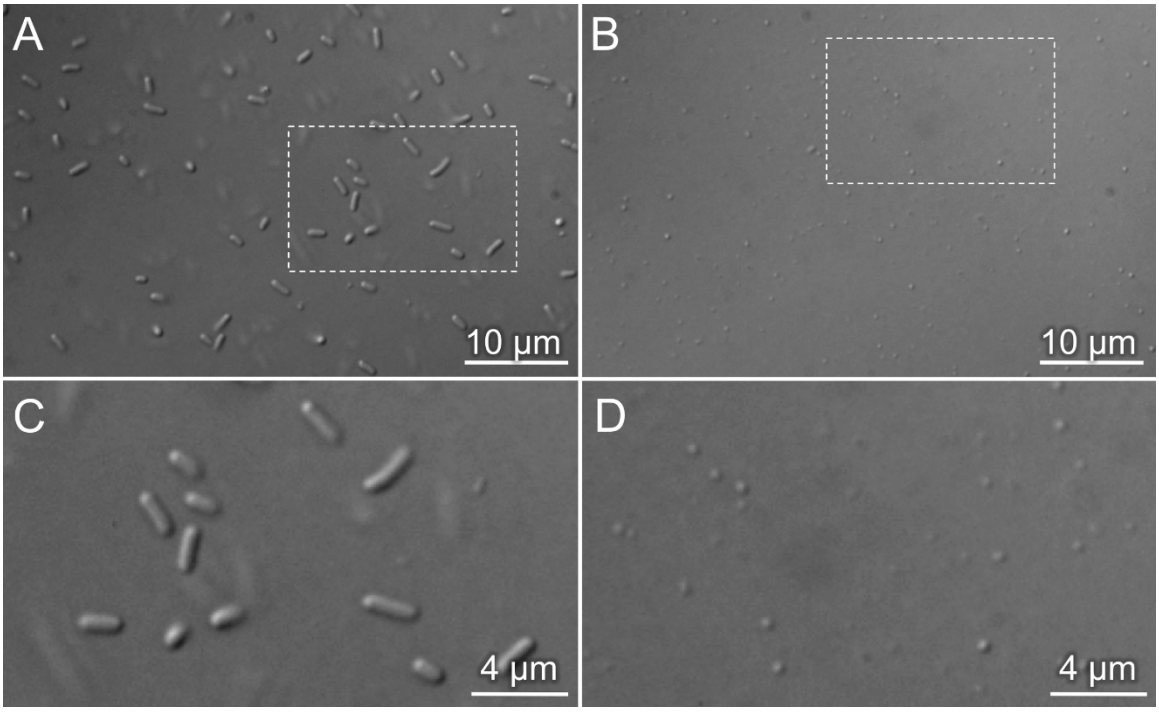

Figure S2. Light microscopy images of normal *S. flexneri* cells (A) and purified minicells (B). The zoom-in images are shown in C and D, respectively.

WT			Minicells		
Mean	SD	N	Mean	SD	N
100	9	3	104.2614	10.6486	3

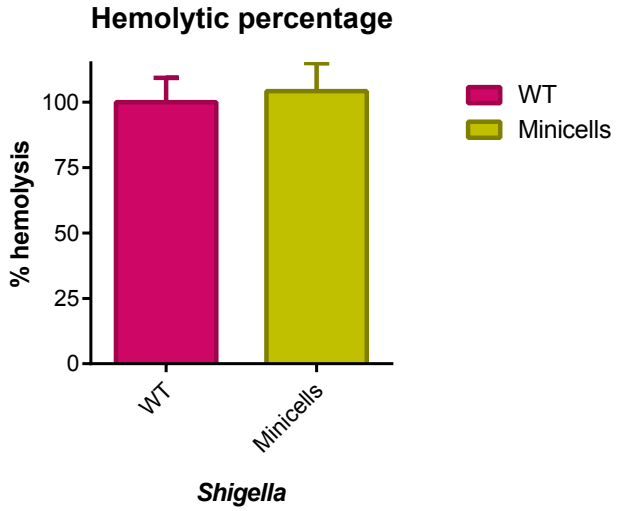

Figure S3. The *S. flexneri* minicells are similar to WT cells in RBC hemolytic activity. The level of hemolysisfor WT *S. flexneri* was normalized to 100%.

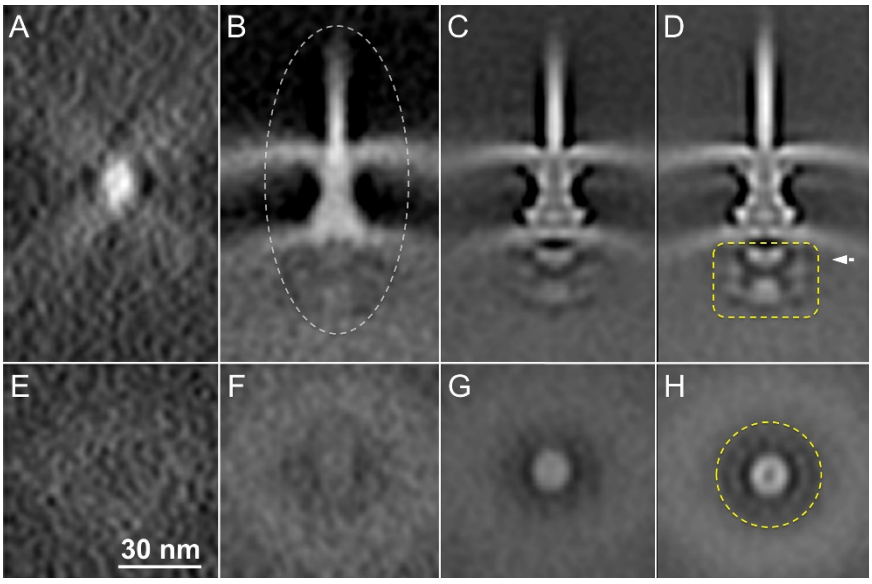

Figure S4. Initial results from sub-tomogram averaging. (A) Initial global average of 4,631 sub-tomograms (the size of each sub-tomogram is 400x400x400 voxels), which were extracted from 387 tomographic reconstructions (3,710 x 3,838 x 1,200). The average is feature-less, because of the random orientation of the injectisomes, however, the initial orientation of each particle can be estimated using the basal body and needle tip coordinates, thereby providing two of the three Euler angles. After applying initial rotation based on two Euler angles, the global average is able to reveal a rough structure of the injectisome embedded in two membranes (B). After several cycles of translational alignment, the global average is significantly improved, and the membranes and the needle are clearly visible (C). Further rotational and translation alignment enhances the global average, in which the cytoplasmic features are visible (white dashed arrow) (D). Comparatively, the cytoplasmic features can be seen in the cross sections E to H, after several cycles of alignment. Importantly, the initial alignment (with 4x4x4 binding and low resolution) is fast and reliable, providing a solid foundation for further classification within a 3-D mask (defined by dashed lines in panels D, H).

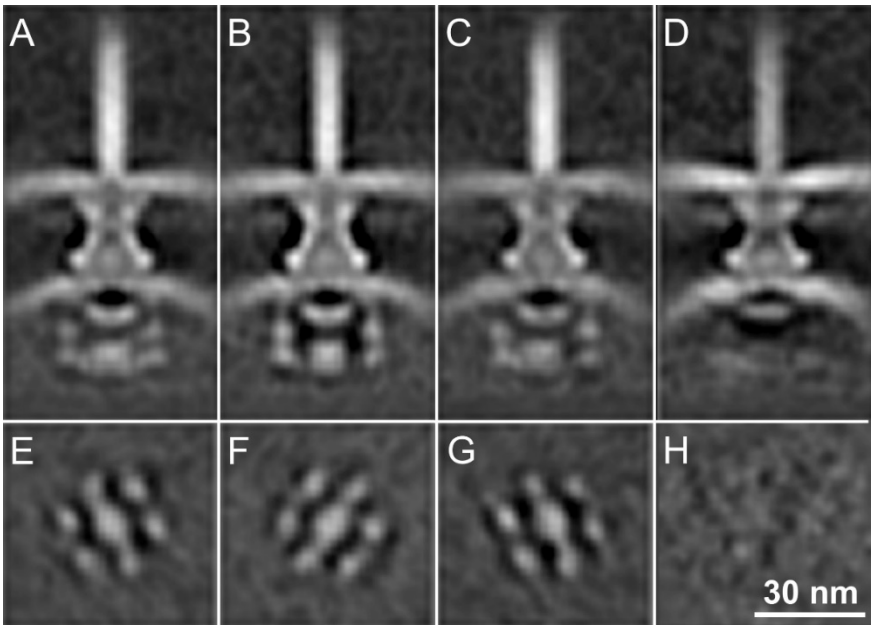

Figure S5. 3-D classification reveals hexagonal features in the cytoplasm. After initial alignment, a binary mask for cytoplasmic area was applied (*SI Appendix*, Fig. S4D, H). Relevant voxels of the aligned sub-tomograms were analyzed by multivariate statistical analysis and hierarchical ascendant classification. Three class averages (A, B, C) of injectisomes from minicells contain hexagonal features in the cytoplasm as shown in the cross-sections (E, F, G) at the bottom of the injectisome. In contrast, the class average of the injectisome from the osmotically shocked cells does not contain the cytoplasmic structure (D, H).

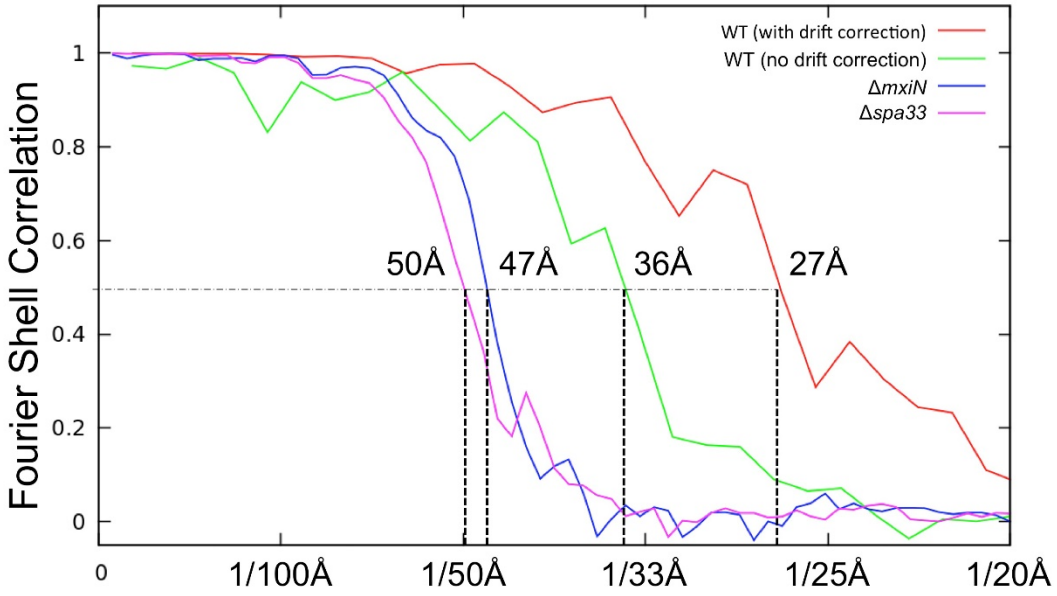

Figure S6. The "gold standard FSC" between the two independent reconstructions was used to estimate the resolution of the averaged structures.

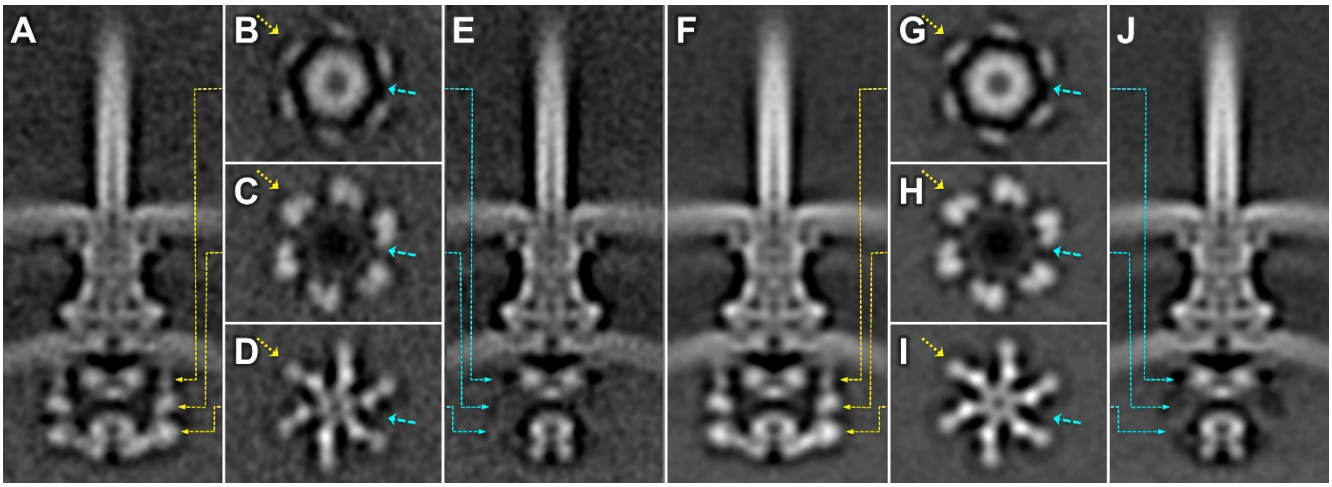

Figure S7. The cytoplasmic complex exhibits hexagonal features. Two central sections (A, E) of the injectisome structure without imposing rotational symmetry reveal a large cytoplasmic complex. The location of the first central section (A) is shown by the yellow arrows corresponding to three cross-sections (B, C, D). The location of the second central section (E) is shown by the cyan arrows corresponding to the same three cross-sections (B, C, D). The hexagonal features of the cytoplasmic complex are apparent in these three different cross-sections (B, C, D). After imposing six-fold symmetry, the two central sections (F, J) and the three cross-sections (G, H, I) are revealed more clearly.

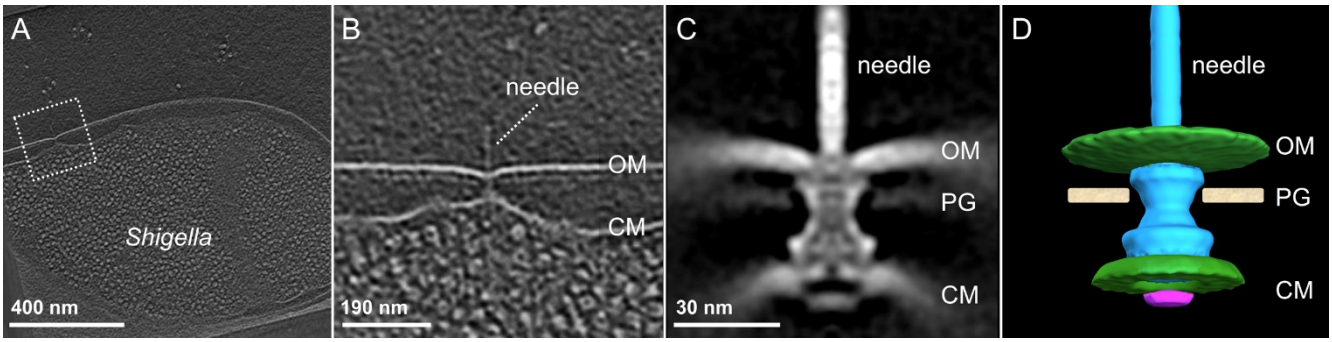

Figure S8. The injectisome structure from osmotically shocked *Shigella* cells. (A) A section from a 3-D tomographic reconstruction of an osmotically shocked cell. One injectisome is shown highlighted in (B). The averaged structure is shown in a central section (C) and a surface view (D). The major portion of the cytoplasmic complex is absent from the T3SS seen in these cells.

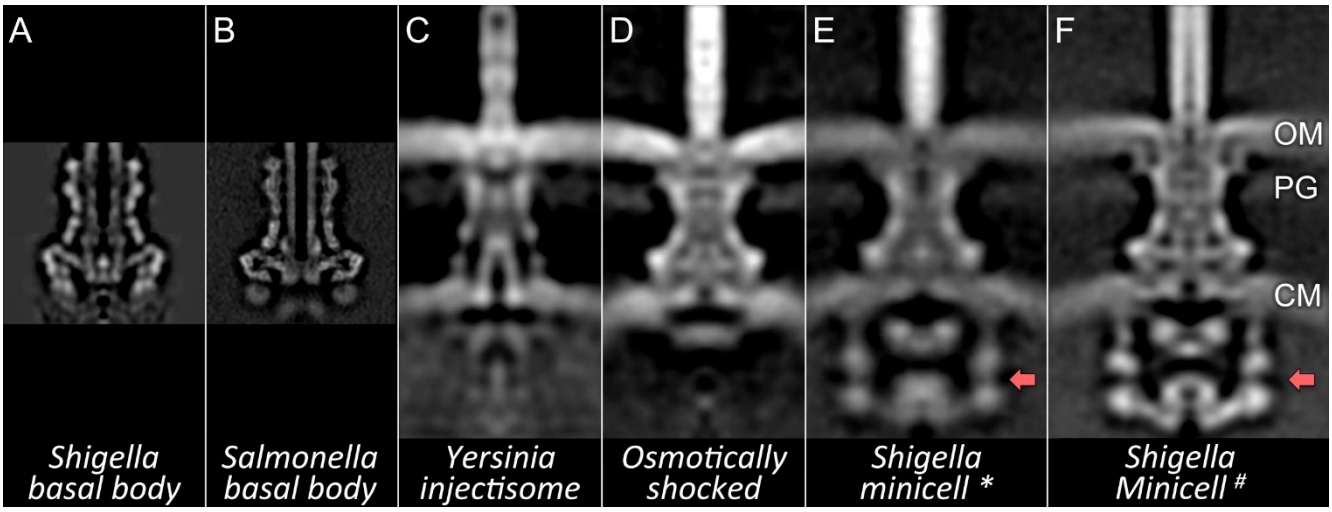

Figure S9. Comparative analysis of available structures reveals the novel cytoplasmic complex in *Shigella* minicells. Central slices of the density maps from (A) the *Shigella* basal body (EMD-1617), (B) the *Salmonella* basal body (EMD-1875), (C) the *in situ Yersinia* whole cell injectisome (EMD-5694), (D) the *Shigella* injectisome from osmotically shocked cells (this study), (E) the intact injectisome (without drift correction and CTF correction) and (F) the intact injectisome from *Shigella* minicells (with drift correction and CTF correction, EMD-2667, this study). The pod structures present in the *Shigella* minicell structure (red arrow) are not visible in the whole cell *Yersinia* injectisome or the osmotically shocked *S. flexneri* cells (D).

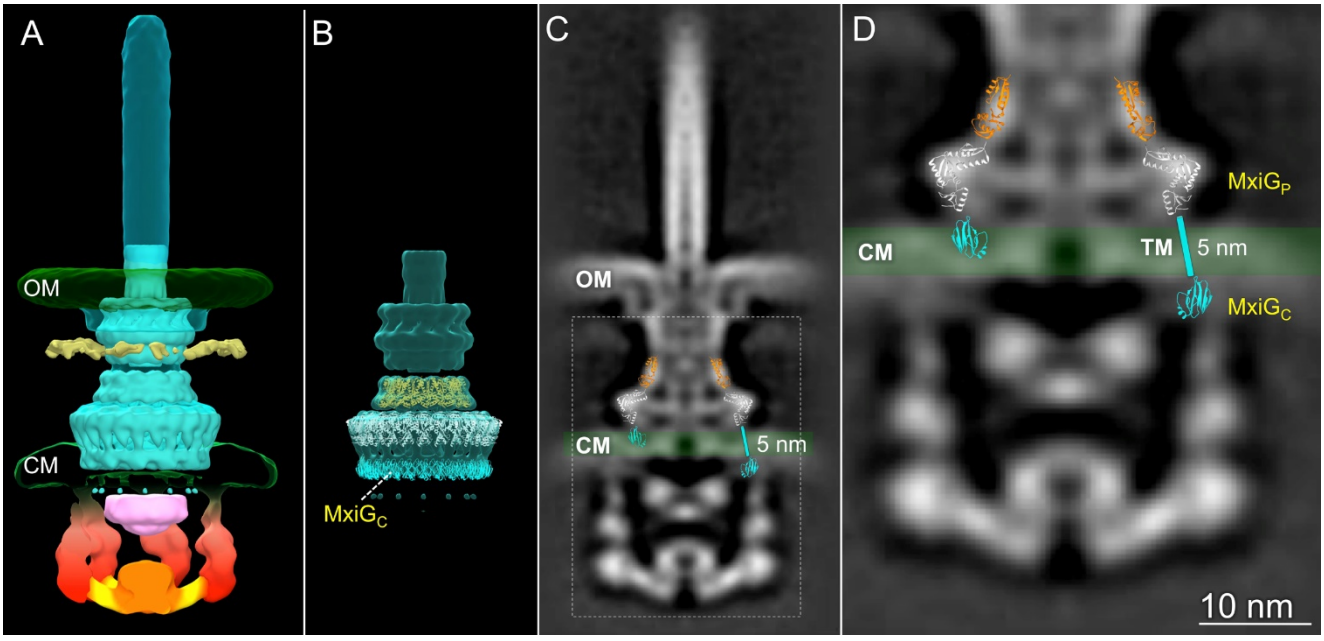

Figure S10. Docking available crystal structures and the high-resolution basal body structure into our map reveals an extended cytoplasmic domain of MxiG. (A) The *Salmonella* needle complex structure (EMD-1875) was fitted into our map. The inset is the EM map with the fitting of InvG (PDB-3J1V), PrgH$_P$ (PDB-3J1X) and PrgH$_C$ (PDB-3J1W). (B) Fitting the atomic structures of InvG, PrgH$_P$ and PrgH$_C$ results in the cytoplasmic domain of PrgH$_C$ localizing to the cytoplasmic membrane (CM) instead of in the cytoplasm (C). To correct this, we built a new model of the cytoplasmic domain of MxiG (MxiGc, the homolog of PrgHc, *SI Appendix*, Table S1) by shifting MxiGc towards the cytoplasm (D).

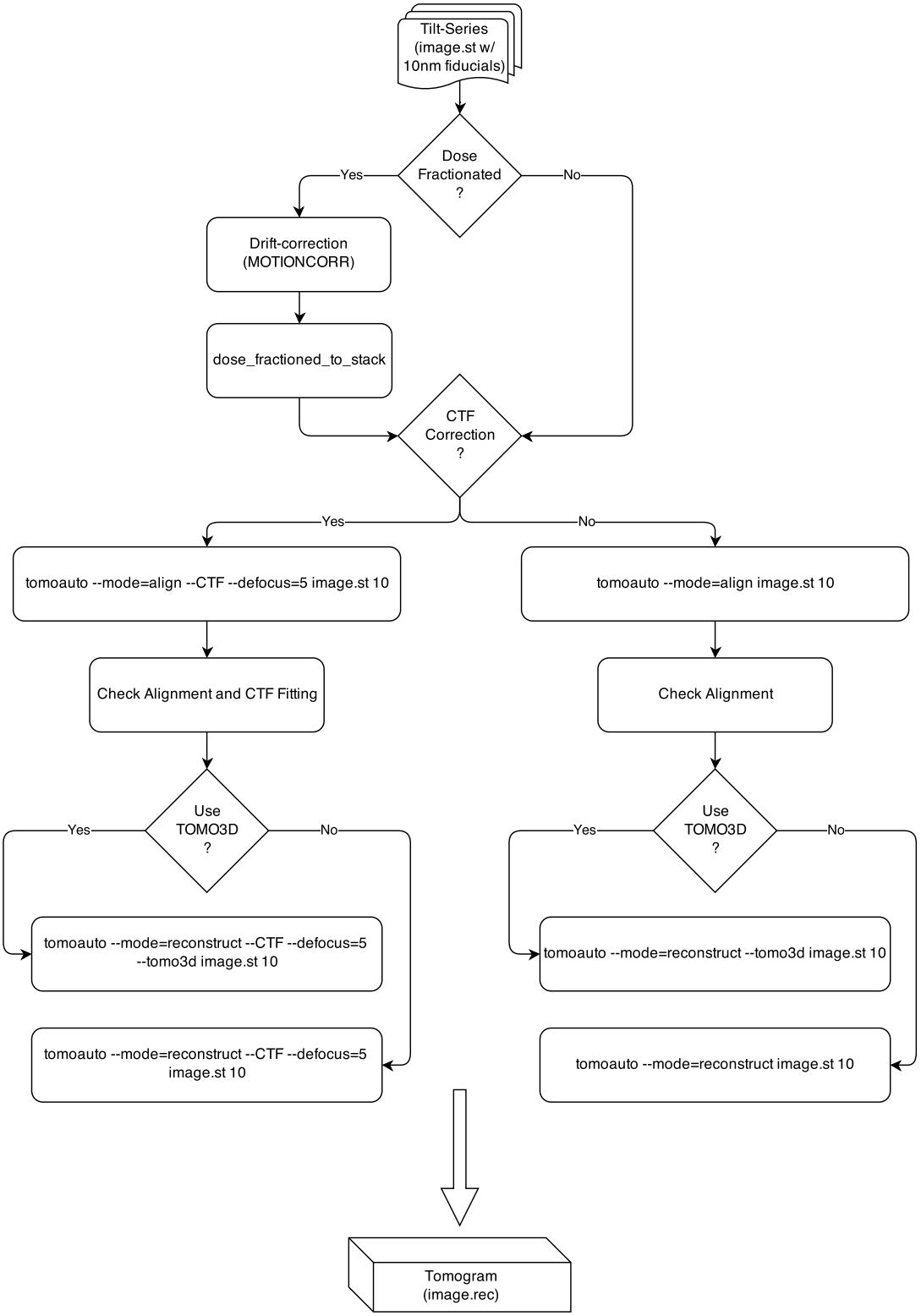

Figure S11. Flowchart from a tilt series to a 3-D reconstruction by using Tomoauto.

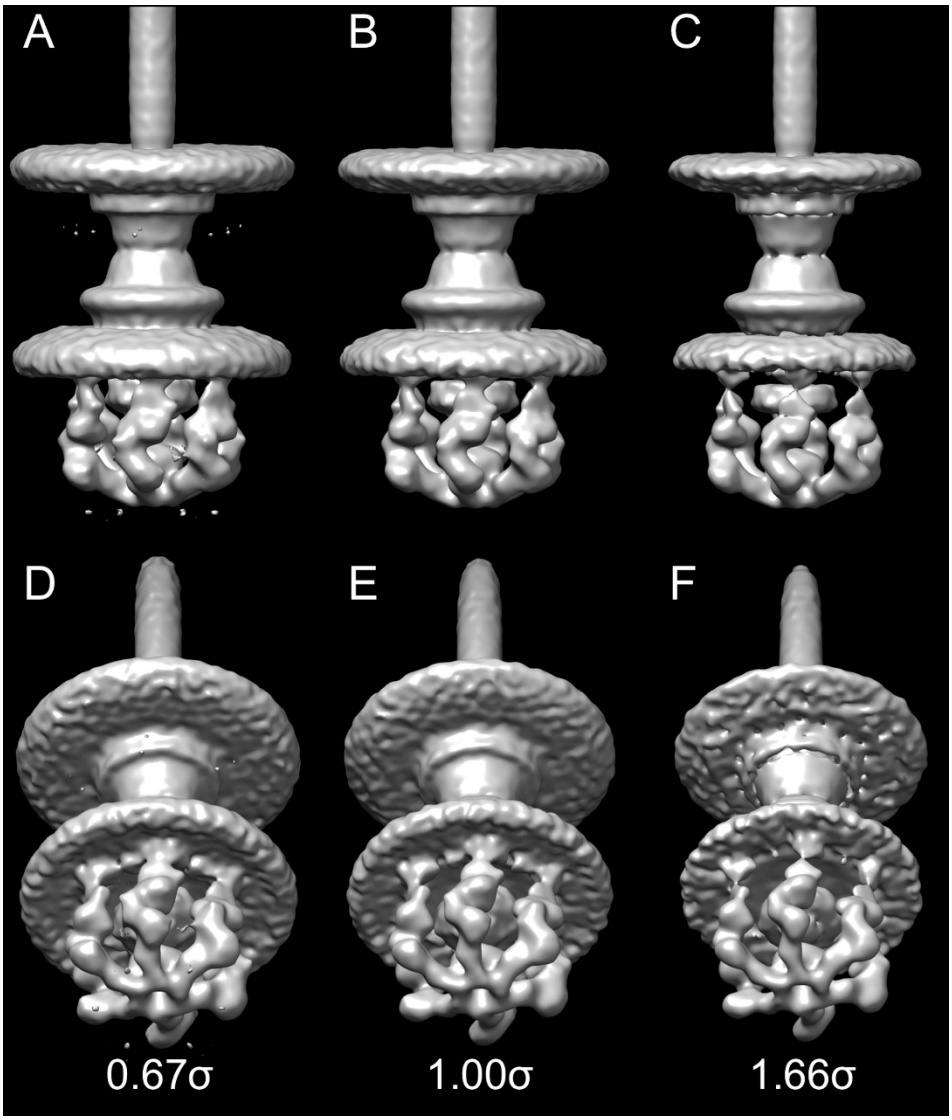

Figure S12. Three isosurface maps are rendered in three different contour levels 0.67σ (A, D), 1.00σ (B, E), and 1.66σ (C, F), respectively. Noticeably, there are extra weak densities underneath the cytoplasmic membrane (D).

Supplementary Movies:

Movie S1. 3-D reconstruction of a *Shigella* minicell derived from the WT strain shows multiple intact injectisomes embedded in the cell envelope.

Movie S2. Cryo-electron tomography of a red blood cell infected by *Shigella* minicells. The injectisome and its medicated minicell-host interaction are shown at high resolution.

Movie S3. An animation showing the transition from initial minicells to molecular architecture of the intact injectisome in *Shigella*. The high-resolution structure is important for understanding of the *Shigella*-host interaction.